UDK 661.865.5:549.282
Original scientific article/Izvirni znanstveni članek

ISSN 1580-2949
MTAEC9, 57(5)537(2023)

SYNTHESIS, CHARACTERIZATION OF CeO_2@Ag HOLLOW SPHERES AND EVALUATION OF THEIR CATALYST ACTIVITY FOR THE REDUCTION OF 4-NP

SINTEZA IN KARAKTERIZACIJA VOTLIH KROGLIC CeO_2@Ag TER OVREDNOTENJE NJIHOVE KATALITIČNE AKTIVNOSTI ZA 4-NP

Shu Cui[1,2], Haixin Zhao[2], Chengyou Liu[3], Hai Yu[1], Nan Li[2*], Xiaotian Li[2*]

[1]Tonghua Normal University, School of Physics, Tonghua, Jilin 134002, China
[2]Jilin University, College of Material Science and Engineering, Key Laboratory of Automobile Materials of Ministry of Education, 2699 Qianjin Street, Changchun 130012, P. R. China
[3]Hainan Vocational University of Science and Technology, School of Chemistry and Materials Engineering, Hainan 570000, China

Prejem rokopisa – received: 2023-03-03; sprejem za objavo – accepted for publication: 2023-08-26

doi:10.17222/mit.2023.813

A CeO_2@Ag hollow spherical composite catalyst was synthesized with the template method. Firstly, a SiO_2@CeO_2 core-shell structure was synthesized using SiO_2 spheres as the template, and then the SiO_2 core was removed by etching to obtain hollow CeO_2 spheres. The CeO_2 hollow microspheres have a large specific surface area, which can effectively suppress the aggregation of Ag nanoparticles, leading to CeO_2@Ag with a regular morphology and well dispersed Ag nanoparticles. There is a strong synergistic effect between CeO_2 and Ag, which is beneficial to improving the catalytic performance. As a result, the CeO_2@Ag hollow spherical composite catalyst can reduce 4-nitrophenol efficiently.

Keywords: CeO_2 hollow spheres, Ag nanoparticles, composite, catalyst activity

Avtorji so sintetizirali kompozitni katalizator na osnovi srebra in cerijevega oksida (CeO_2@Ag) v obliki votlih kroglic sšablonsko metodo. Najprej so za jedro lupinaste strukture SiO_2@CeO_2uporabili SiO_2 kroglice in nato so SiO_2jedro odstranili z jedkanjem ter tako dobili samo CeO_2mikro kroglice. Te imajo veliko specifično površino in presek, ki učinkovito zavira skupljanje srebrnih nanodelcev. To je omogočilo izdelavo kompozita CeO_2@Ag s pravilno morfologijo in dobro porazdelitvijo nanodelcev srebra (Ag) na površini kroglic. Pri tem je prišlo do močnega sinergijskega (obojestranskega) delovanja med CeO_2in Ag, karje močno izboljšalo katalitične učinke tega kompozita. Avtorji v zaključku povdarjajo, da so izdelali kompozitni katalizator iz votlih mikrokroglic CeO_2@Ag, ki močno zmanjšujeučinkovitost 4-nitrofenola (p-nitrofenol ali 4-hidroksinitrobenzen), ki se v industriji uporablja za izdelavo zdravil, fungicidov, insekticidov, barv, za temnjenje usnja itd.

Ključne besede: votle kroglice CeO_2, nanodelci srebra, kompozit,katalitična aktivnost

1 INTRODUCTION

Noble metal nanomaterials have extensive potential applications in catalysis, antibacterial, electrochemistry, sensors, etc. Compared to other noble metal nanomaterials, Ag nanoparticles (AgNPs) have a relatively low price and distinctive catalytic capability, thus they have received increasing attention in the field of catalysis, relating to catalytic oxidation,[1,2] catalytic reduction[3,4] or catalytic selection.[5,6] Numerous studies[7–9] showed that small-sized and monodispersed AgNPs usually exhibit a high catalytic activity. Nevertheless, individual AgNPs frequently tend to accumulate during a synthesis process, reducing the catalytic performance.[10–12] In order to solve this problem, an effective method is a recombination of AgNPs on/in nanostructured solid substrates, for instance, silica,[13] carbon,[14] polymer,[15] metal oxides,[16–18] etc.

Among various AgNP supporting materials, ceric oxides have received more attention for their excellent redox properties and high oxygen storage capacity. In Ag@CeO_2 composite catalysts, the synergistic effect between CeO_2 and AgNPs can improve the reduction and oxidization according to some researchers.[19–21] For example, Shi et al.[20] prepared Ag@CeO_2 core-shell nanocomposites through a self-assembly process and investigated the catalytic activity used for the hydrogenation of 4-nitrophenol (4-NP) and 2-nitroaniline (2-NA). The results demonstrated that the Ag@CeO_2 catalysts have outstanding catalytic efficiency and cyclic stability. In another study, Wang et al.[21] synthesized Ag@CeO_2 core-shell nanospheres via a facile one-step solvothermal route using $Ce(NO_3)_3{\cdot}6H_2O$, $AgNO_3$, poly(N-vinylpyrrolidone) (PVP) and ethanol. The enhanced catalytic activity is found to be due to the unique oxidized Ag species induced by the strong interaction between the core surfaces of Ag nanospheres and surface defects (oxygen vacancies) of the CeO_2 shell.

Hollow CeO_2 nanostructures have been used in many applications, such as photocatalytic water oxidation, catalytic reduction, sensors, etc. A high dispersibility and

*Corresponding author's e-mail:
xiaotianli@jlu.edu.cn(X. Li)

large specific surface area often result in better performance. Despite several studies, a controlled synthesis of CeO_2 hollow nanostructures for catalysts has still been limited. In this work, we synthesized CeO_2 hollow mesoporous spherical supported AgNP catalysts using the template method. The CeO_2 supports have a large specific surface area and mesoporous structure, which can effectively suppress the aggregation of Ag nanoparticles, leading to CeO_2@Ag with a regular morphology and well dispersed Ag nanoparticles. Furthermore, there is a strong synergistic effect between CeO_2 and Ag, which is conducive to improving the catalytic performance.

2 EXPERIMENT SECTION

2.1 Synthesis

The entire fabrication of the CeO_2@Ag hollow microspheres is illustrated in **Figure 1** and detailed information of each step is depicted below.

SiO_2 nanospheres: SiO_2 nanospheres were synthesized with a modified Stöber method following the procedure reported in the literature.[22] Briefly, 64 mL isopropanol and 24 mL deionized water were mixed uniformly, and 13 mL ammonia hydroxide (25–28 *w*/%) were added; they were mixed at 35 °C for 15 min. Then, 0.6 mL tetraethoxysilane (TEOS) was added, and after mixing for 30 min, 5 mL TEOS were added to the mixture, which was stirred for another 2 h. SiO_2 particles were centrifuged from the milky mixture, and then dried at 60 °C for 24 h.

CeO_2 hollow spheres: Primarily, an SiO_2@CeO_2 core-shell composite was prepared using SiO_2 as the template.[23] Briefly, 0.277 g cerium nitrate and 0.07 g methenamine were respectively dissolved in 5 mL deionized water, forming two aqueous solutions. 1 g polyvinyl pyrrolidone (PVP, K29/32) was dissolved in 40 mL deionized water, and 0.1 g of the as-prepared SiO_2 nanospheres was introduced and completely dispersed with ultrasonication, then the mixture was heated to 95 °C in an oil bath. The cerium nitrate solution and methenamine solution were added dropwise into the mixture under vigorous stirring. After 2 h, the gray-white mixture was naturally cooled down, centrifuged, washed (with ethanol and deionized water) and dried at 80 °C. Products were calcinated in a tube furnace at 600 °C for 2 h to obtain light yellow SiO_2@CeO_2 composites. Eventually, to achieve hollow mesoporous CeO_2 nanospheres, the SiO_2@CeO_2 composites were dispersed in a 40 mL NaOH solution (0.2 M) and stirred for 24 h to remove the SiO_2 template.

CeO_2@Ag hollow spheres: Ag nanoparticles on CeO_2 hollow mesoporous nanospheres were fabricated with a simple in situ wet chemistry method as described previously.[24] Briefly, 0.1 g CeO_2 hollow mesoporous nanospheres was dispersed into a 10 mL 5×10^{-5} M silver-ammonia ($[Ag(NH_3)_2]NO_3$) solution with ultrasonication, then stirred at 60 °C for 30 min. 12 g ethanol containing 0.1 g PVP were added dropwise into the suspension, and stirred for 1 h. Finally, the CeO_2@Ag hollow spheres were centrifuged and then dried at 80 °C. The obtained product was denoted as CeO_2@Ag-1. In control experiments, CeO_2@Ag-2 and CeO_2@Ag-3 were prepared with the same method where the concentrations of $[Ag(NH_3)_2]NO_3$ were 1×10^{-4} M and 1.5×10^{-4} M, respectively.

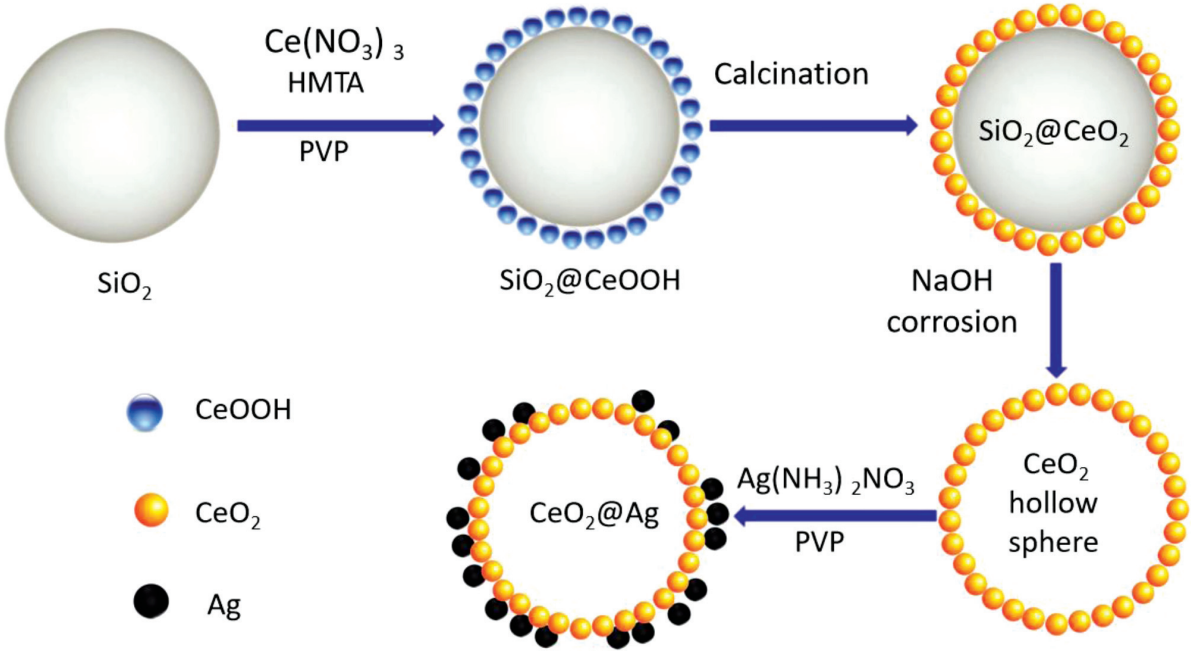

Figure 1: Schematic diagram of the fabrication of CeO_2@Ag hollow microspheres

2.2 Catalyzed reduction of 4-NP

The catalytic activity of the as-prepared catalysts was studied with 4-NP. A mixture of 0.3 mL 4-NP aqueous solution (10 mM) and 3 mL fresh $NaBH_4$ solution (10 mM) was stirred thoroughly. Then 1 mg CeO_2@Ag nanocomposite was added to the mixture, and the catalytic reactions occurred rapidly. The reduction process was analyzed with a UV-Vis spectrophotometer at 90 s intervals.

2.3 Characterization

The crystalline nature was studied with a D8 Tools X-ray diffractometer equipped with Cu K_α (λ = 0.15405 nm). The morphology and microstructure of the synthesized nanomaterials were investigated with a field-emission scanning electron microscope (FESEM/EDS, JEOL JSM-6700F) and transmission electron microscope (TEM, JEM 3010 and Tecnai G2 F20). The binding energies of the elements in the synthesized nanomaterials were measured using X-ray photoelectron spectroscopy (XPS, VG ADES-400). The porosity of the samples was analyzed at 77 K based on nitrogen adsorption-desorption using the Barrett–Joyner–Halenda (BJH) method on a Quantochrome Autosorb 1 sorption analyzer. The Brunauer–Emmett–Teller (BET) measurement was used to determine the specific surface area. UV–Vis diffuse reflectance spectroscopy (DRUV-VIS) of the resultant samples was performed. A Bws003 spectrophotometer operating in a range of 250–650 nm was used to record UV–Vis diffuse reflectance spectra (DRS), while $BaSO_4$ was used as the reference standard.

3 RESULTS AND DISCUSSION

3.1 Characterization

XRD patterns of SiO_2@CeO_2, hollow mesoporous CeO_2, CeO_2@Ag-1, and CeO_2@Ag-2 are presented in **Figure 2**. It can be clearly seen that all the samples have similar characteristic peaks, recognized to be cubic CeO_2(JCPDS 34-0394).[25] Diffraction peaks at 2θ = 28.6°, 33.2°, 47.6° and 56.3° can be indexed to the (111), (200), (220) and (311) crystal faces of cubic CeO_2. Diffraction peaks are obviously broad, indicating that the size of CeO_2 crystallites is very small. According to the Scheler formula, the size of CeO_2 crystallites is about 5.6 nm. For CeO_2@Ag-1, there is a weak diffraction peak near 37.9°, corresponding to the face centered cubic structure of Ag (JCPDS 4-783),[24] indicating that AgNPs are successfully loaded on CeO_2 hollow spheres. The characteristic peak of Ag is obviously wide, indicating that the size of Ag crystallites is very small. In sample CeO_2@Ag-2, the characteristic peak of Ag has been enhanced, but it is still relatively wide.

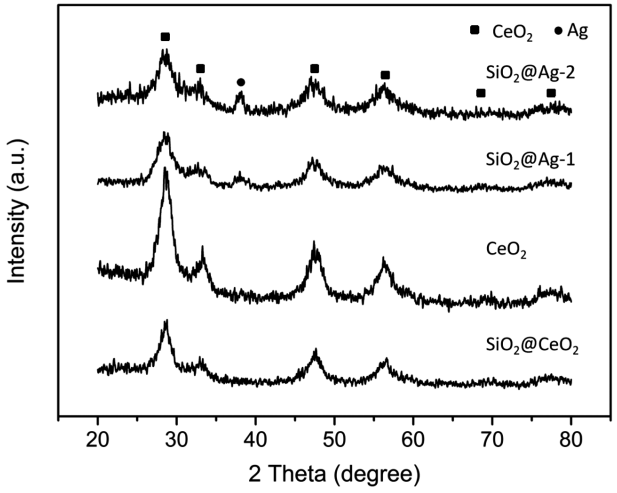

Figure 2: XRD patterns of the samples

Figure 3 shows FESEM images of the prepared products in each stage. As shown in **Figure 3a**, the SiO_2 spheres exhibit regular spherical shapes with a uniform size distribution and good dispersion, and the average diameter is 170 nm. After applying CeO_2 (**Figure 3b**), the shape and dispersity of SiO_2@CeO_2 core-shell composites did not change obviously, but the surfaces of the spheres became rough, and the average diameter increased to 185 nm. After the SiO_2 spherical cores are corroded by NaOH, there are hollow CeO_2 spheres, shown in **Figure 3c**. It can be seen that the sample still maintains a regular spherical morphology. A few broken spherical shells clearly show the hollow structure, and the spherical shells are very thin. As shown in **Figures 3d** to **3f**, the Ag loaded CeO_2 hollow spheres have a similar spherical morphology, indicating that the CeO_2 shell is relatively stable and the diameter of the CeO_2@Ag samples is not changed obviously. However, the surface of the samples becomes rougher and there are some nanoparticles of less than 10 nm on the surface.

Based on the above and the previous XRD results, we can infer that these small particles are AgNPs. For CeO_2@Ag-1 (**Figure 3d**) and CeO_2@Ag-2 (**Figure 3e**), the nanoparticles are uniformly adhered to the surface of spheres; as the concentration of $[Ag(NH_3)_2]NO_3$ increases from 5×10^{-5} M to 1×10^{-4} M there are no distinct morphological differences between the two samples. But for CeO_2@Ag-3 (**Figure 3f**), when the concentration of $[Ag(NH_3)_2]NO_3$ increases to 1.5×10^{-4} M there is a cuboid particle with a size of 450 nm, marked with a red dashed circle, and the morphology is obviously different from the spherical morphology of the CeO_2@Ag samples. This cuboid formation could be an Ag particle, indicating that with a high concentration of $[Ag(NH_3)_2]NO_3$, the AgNPs tend to agglomerate and form large-size silver particles, affecting the catalytic activity of CeO_2@Ag-3.

To further study the microstructures and AgNP distribution of CeO_2@Ag hollow spheres, CeO_2@Ag-2 was observed with TEM and HRTEM. It can be clearly seen on **Figure 4a** that the CeO_2@Ag microspheres have an obvious hollow structure. The average diameter of the

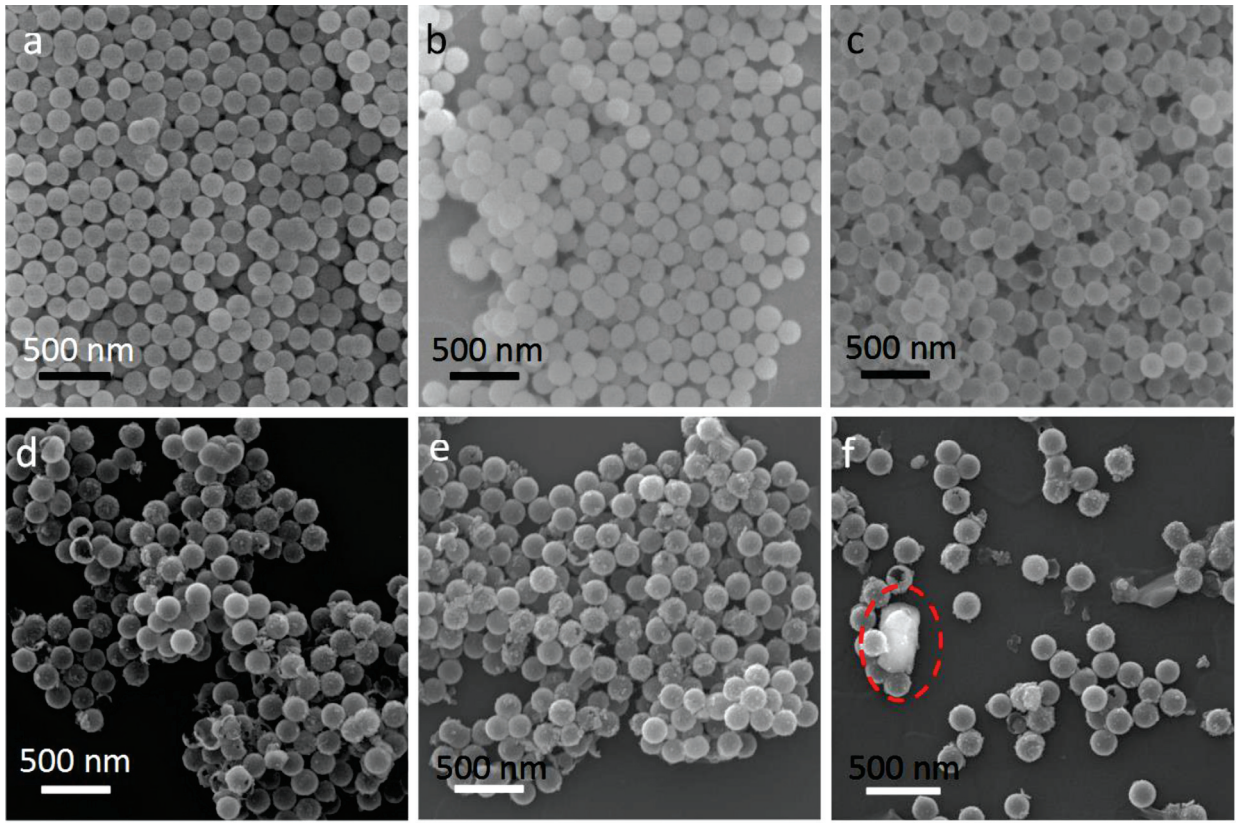

Figure 3: a) FESEM images of the as-prepared samples: SiO_2 spheres, b) SiO_2@ CeO_2 core-shell composites, c) CeO_2 hollow microspheres, d) CeO_2@Ag-1, e) CeO_2@Ag-2, f) CeO_2@Ag-3

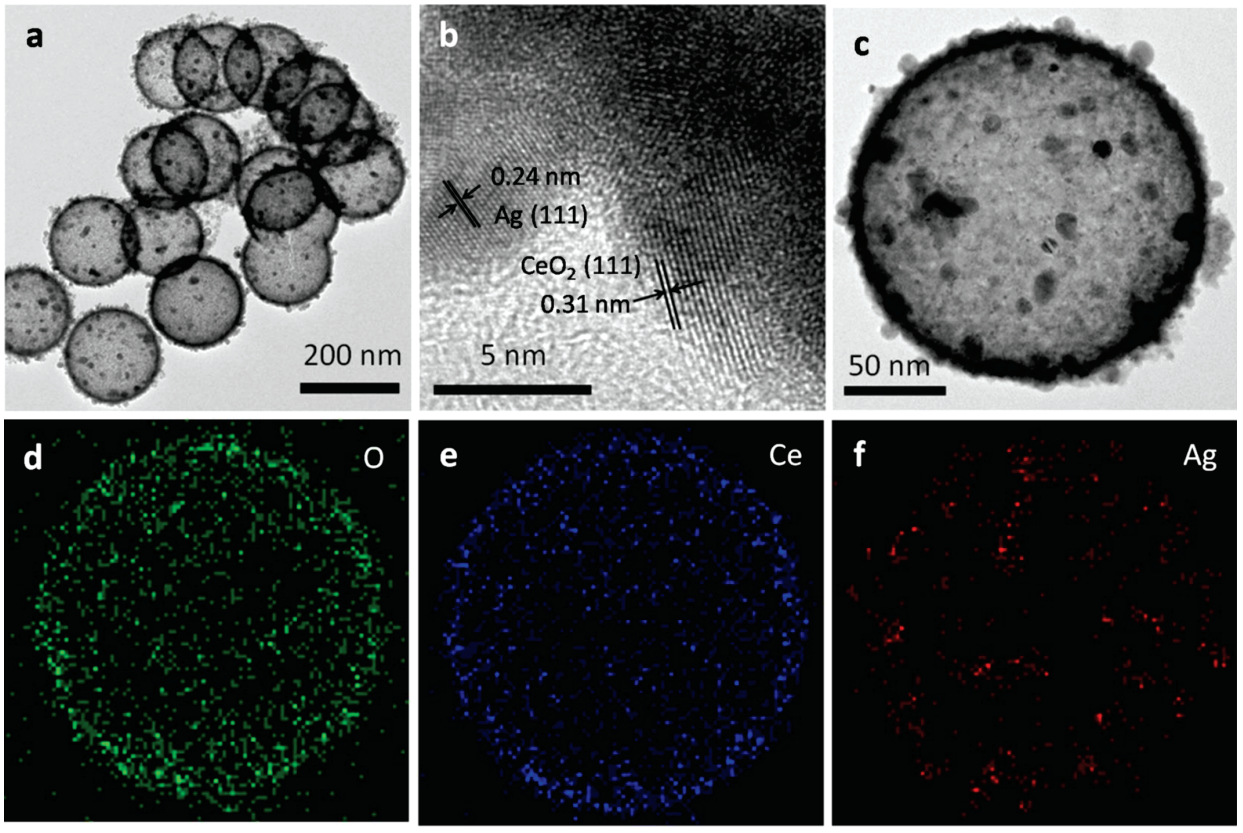

Figure 4: a, b, c) TEM images of CeO_2@Ag-2 hollow microspheres, d–f) the elemental mapping of a CeO_2@Ag-2 hollow monomicrosphere

hollow spheres is 180 nm, and the thickness of the shell is about 7 nm, which is consistent with the SEM results. The light and shade contrast shows that there are some small and well dispersed nanoparticles on the surface of the spherical shell, with a size of ~10 nm. In the HRTEM image of **Figure 4b**, clear lattice fringes can be seen. After measurement, there are two different lattice fringes with a distance of 0.24 nm and 0.31 nm that can be indexed to the (111) plane of the face centered cubic structure of Ag (JCPDS 4-783) and (111) plane of the cubic structure of CeO_2(JCPDS 34-0394).[26] An elemental mapping analysis (**Figures 4e** and **4f**) of a single CeO_2@Ag-2 hollow microsphere (**Figure 4d**) indicates the existence of Ce, O and Ag. **Figure 4f** demonstrates that AgNPs are homogeneously dispersed in the whole CeO_2@Ag-2 hollow microsphere.

To qualitatively determine the surface compositions and elemental chemical status of the CeO_2@Ag hollow microspheres, CeO_2 and CeO_2@Ag-2 were investigated using the XPS analysis. **Figure 5a** shows the full spectrum in a range of 0–1200 eV of the two samples; Si, C, O and Ce signals are observed in both curves. The C signal results from the carbon calibration.[27] The Si signal is weak, resulting from the residual of the SiO_2 core in the sample. The intensity of the Ce signal did not change after loading AgNPs, indicating that the loading amount of AgNPs was very small; the coverage area of nano-AgNPs on the surfaces of the CeO_2 hollow microspheres was very low, and there was still a large area of the CeO_2 shell exposed on the sample surface. The Na signal in the curve of the CeO_2 sample is attributed to the residual NaOH used to remove the SiO_2 core. In the curve of CeO_2@Ag-2, there is an obvious Ag signal. **Figure 5b** shows the high-resolution XPS spectra of Ag 3d. The two characteristic peaks located at 368.2 eV and 374.2 eV correspond to the binding energies of Ag 3d5/2 and Ag 3d3/2, respectively,[28] indicating that Ag exists as Ag^0 on the surface. This further confirms the existence of AgNPs in the CeO_2@Ag-2 sample. The high-resolution XPS spectrum of Ce 3d, shown in **Figure 5c**, has two characteristic peaks located near 883.8 eV and 902.2 eV that are attributed to the binding energies of Ce 3d5/2 and Ce 3d3/2,[28] indicating that Ce exists as Ce^{4+}. **Figure 5d** shows the high-resolution XPS spectrum of O 1s. The two characteristic peaks located near 529.4 eV and 531.7 eV belong to the lattice oxygen and surface chemisorbed oxygen O 1s.[29]

In order to further clarify the surface areas and mesoporous structures of CeO_2 and CeO_2@Ag hollow spheres, nitrogen sorption experiments were carried out. It can be seen from **Figure 6** that the shape of both isotherms is a typical type IV curve, with an obvious H1

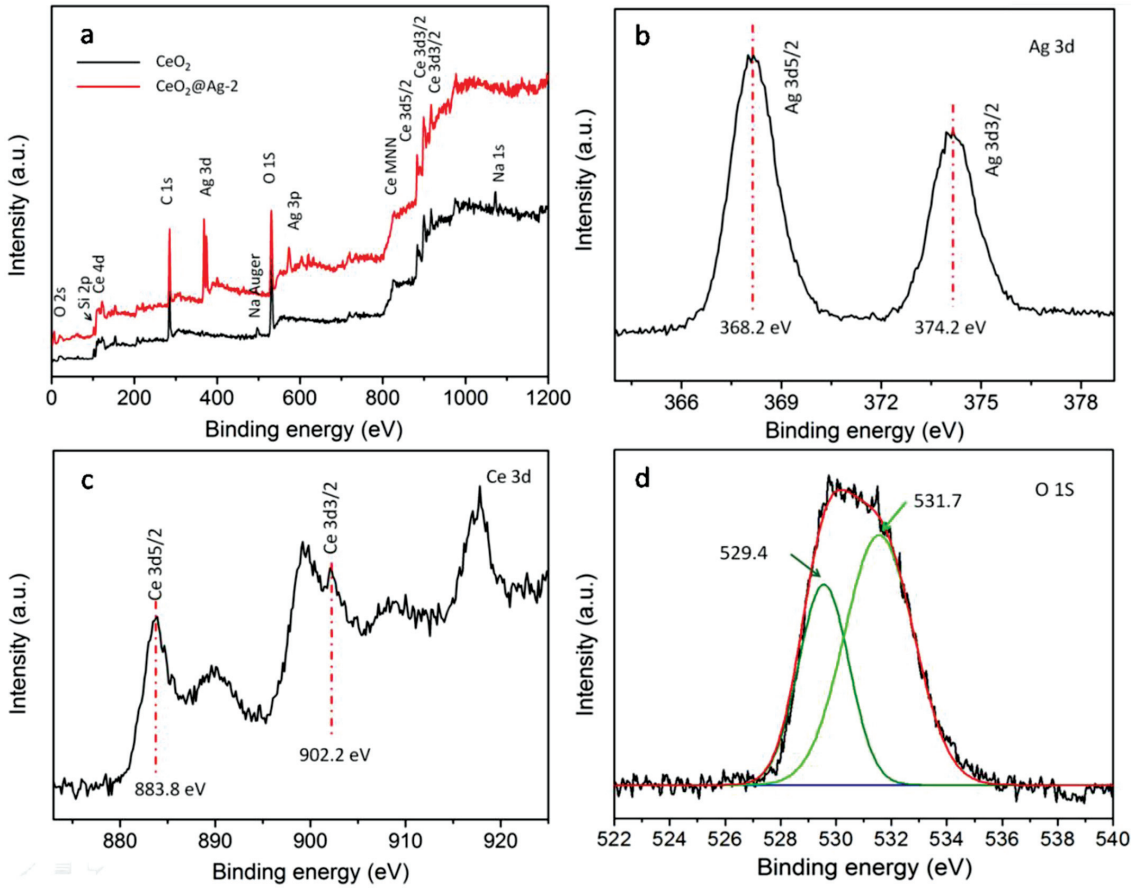

Figure 5: a) XPS survey of CeO_2 and CeO_2@Ag-2, b) XP spectra of CeO_2@Ag-2: Ag 3d, c) Ce 3d, d) O 1s

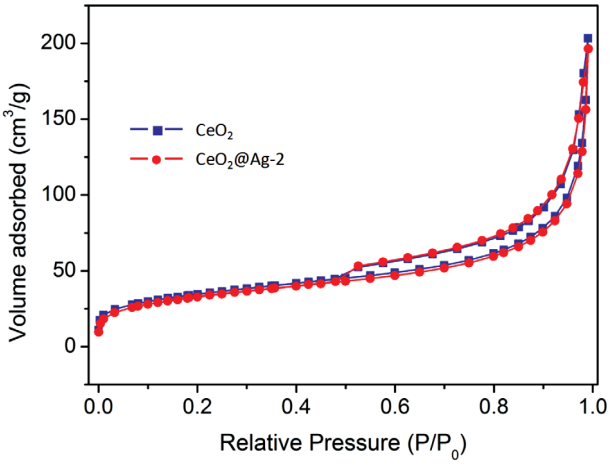

Figure 6: Nitrogen adsorption–desorption isotherm of CeO_2 and CeO_2@Ag-2

hysteresis loop, indicating that CeO_2 and CeO_2@Ag-2 have mesoporous properties, which mainly arise from the accumulation of CeO_2 nanoparticles. The hysteresis loops of CeO_2 and CeO_2@Ag-2 are almost the same. According to the results of SEM and TEM, Ag is mainly distributed on the surfaces of CeO_2 hollow microspheres, so it has little effect on the accumulation of CeO_2 grains in the shell. The specific surface areas of CeO_2 and CeO_2@Ag-2 are 122.4 cm^2/g and 117.0 cm^2/g, respectively, resulting from the hollow structures of the samples. This result is much higher than in similar cases reported in the literature, which are listed in **Table 1**. Such a high specific surface area is conducive to the adsorption and catalytic reaction of pollutants.

Table 1: Comparison of specific surface areas based on various CeO_2 hollow nanostructures

Catalyst	Specific surface area	References
CeO_2 hollow spheres	67.16 (cm^2/g)	30
CeO_2 hollow spheres	67.1 (cm^2/g)	31
CeO_2 hollow spheres with a tunable pore structure	32.266 ~ 54.668 (cm^2/g)	32
CeO_2 hollow spheres	122.4 (cm^2/g)	This work
CeO_2@Ag-2	117.0 (cm^2/g)	This work

3.2 Catalytic activity for the catalytic reduction of 4-NP

4-NP is an organic pollutant widely existing in industrial wastewater. It is highly soluble and difficult to be naturally degraded. Nobel metal catalysis is an effective green method for dealing with this problem. Therefore, we chose 4-NP as the degradation target to evaluate the catalytic activity of as-prepared CeO_2@Ag, and the results are shown in **Figure 7**. **Figure 7a** shows the absorption spectrum of 4-NP. Two obvious absorption peaks can be seen, one is near 400 nm and the other is near 300 nm, corresponding to 4-NP and 4-aminophenol

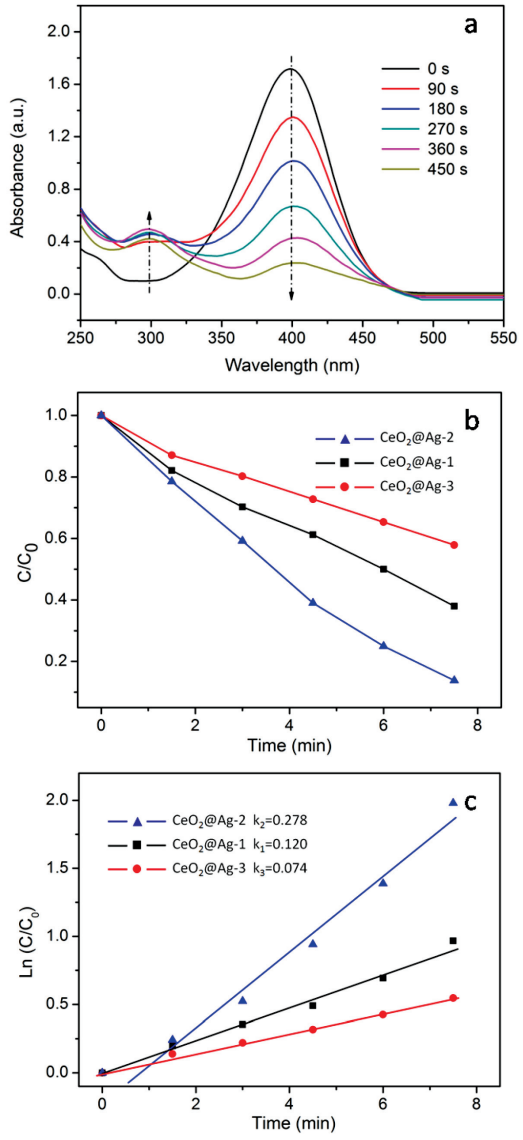

Figure 7: a) Absorption spectra of 4-NP in the presence of CeO_2@Ag-2, b) catalytic reduction of 4-NP by different CeO_2@Ag samples, c) corresponding curves between $\ln(C/C_0)$ and reduction time

(4-AP). Generally, the conversion of aromatic nitro compounds into aromatic amino compounds is an important step in organic chemical synthesis and industrial production.[33] With a catalytic time from 0 to 450 s, a strong absorption peak corresponding to 4-NP decreases rapidly, while the absorption peak corresponding to 4-AP increases gradually, indicating that 4-NP was rapidly reduced to 4-AP under the effect of the CeO_2@Ag-2 catalyst. The catalytic reduction rate was 86 % at 450 s, indicating that the CeO_2@Ag-2 catalyst is very effective for the catalytic reduction of 4-NP.

The catalytic reduction curves of C/C_0 versus catalytic time for the CeO_2@Ag samples are plotted in **Figure 7b** where C_0 is the initial concentration of 4-NP and C is the real-time concentration. After 450 s, the catalytic reduction efficiencies for CeO_2@Ag-1,

CeO_2@Ag-2 and CeO_2@Ag-3 were (62, 86 and 42) %, respectively. Thus, CeO_2@Ag-2 exhibits the best performance. **Figure 7c** shows the corresponding $\ln(C/C_0)$ curves. All the curves of the three CeO_2@Ag samples show the Langmuir-Hinshelwood first-order kinetics model.[34] As calculated, the rate constants are 0.120, 0.278 and 0.074 for CeO_2@Ag-1, CeO_2@Ag-2 and CeO_2@Ag-3. Obviously, with the increase in the Ag loading, the catalytic performance of the series of samples increased first and then decreased; CeO_2@Ag-2 showed the best catalytic performance.

To further analyze the difference in the catalytic performance of CeO_2@Ag catalysts, we carried out a UV–Vis diffuse reflectance test, and the result is shown in **Figure 8**. It can be seen that all the samples have an obvious absorption edge near 400 nm, corresponding to the band gap width of CeO_2.[33] After loading AgNPs, the absorption of CeO_2@Ag catalysts in the visible region is enhanced, as described in the literature,[33,35] which can be generally attributed to the interaction between electrons in CeO_2 and AgNPs, leading to more oxygen vacancies. CeO_2@Ag-2 has the strongest absorption in the visible region, so we infer that the synergistic effect between CeO_2 and AgNPs is also the strongest.

According to the previous SEM results, with the concentration of $[Ag(NH_3)_2]NO_3$ solution increasing from 5 × 10^{-5} M to 1 × 10^{-4} M, AgNPs can be well dispersed on the surfaces of CeO_2 hollow spheres and the grain size is less than 10 nm. The synergistic effect between AgNPs and CeO_2 benefits the catalytic activity of AgNPs in the catalytic process, so the CeO_2@Ag-2 sample with the higher Ag loading amount exhibits the best performance. When the concentration of the $[Ag(NH_3)_2]NO_3$ solution increases to 1.5 × 10^{-4} M, the concentration of silver ions is too high; they are rapidly reduced to AgNPs in the solution and then agglomerated to large-size silver particles which have a poor catalytic ability. As a result, the amount of the silver ions adsorbed on the CeO_2 hollow spheres is reduced, and the synergistic effect between AgNPs and CeO_2 is weakened; both reasons lead to a decreased catalytic performance of the CeO_2@Ag-3 sample. On the one hand, for our prepared CeO_2@Ag catalysts, the CeO_2 hollow sphere framework provides a carrier with a large specific surface area for AgNPs, which is conductive to controlling the size of AgNPs and increasing the effective area of AgNPs in the catalytic process. On the other hand, the synergistic effect between CeO_2 and AgNPs is affected by the loading amount of Ag. Excessive loading will not only cause a waste of raw materials, but also reduce the catalytic efficiency. As a result, the CeO_2@Ag hollow composite catalysts can show the best catalytic performance only at the optimum loading amount of Ag.

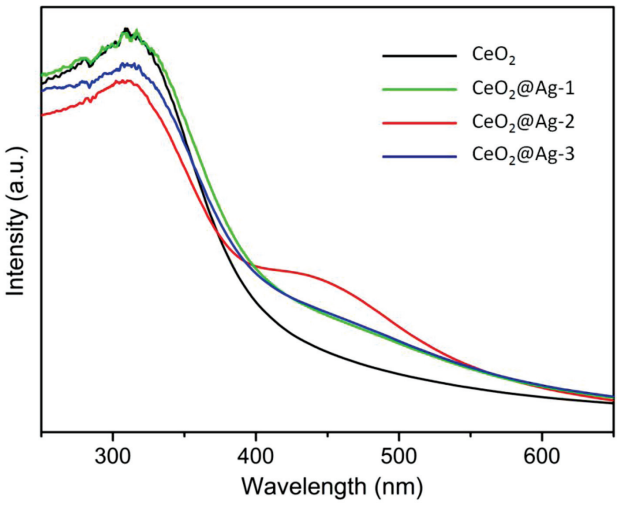

Figure 8: UV-Vis absorption spectra of the samples

4 CONCLUSIONS

In summary, we successfully prepared a CeO_2@Ag hollow spherical composite catalyst using the template method. The specific surface area of CeO_2 hollow microspheres is up to 122.4 cm^2/g, which is higher than that of similar CeO_2 hollow microspheres found in the literature. The mesoporous structure of CeO_2 hollow microspheres plays a key role in controlling the size and dispersion of AgNPs. The grain size of the AgNPs on the surfaces of CeO_2 hollow microspheres is less than 10 nm, and the specific surface area of the CeO_2@Ag-2 catalyst is 117.0 cm^2/g. In the study of the catalytic performance for the reduction of 4-NP, the as-prepared CeO_2@Ag-2 sample exhibits the best catalytic efficiency of 86 % at 450 s. This excellent catalytic performance is attributed to the small grain size of AgNPs controlled by the CeO_2 hollow mesoporous structure and the synergistic effect between CeO_2 and AgNPs. The preparation method for metal@oxide hollow spheres can be used in the synthesis of many other materials, and this CeO_2@Ag composite material can also be used in many other application fields.

Acknowledgements

This work was supported by the National Natural Science Foundation of China (No. 21076094), the Educational Commission of the Jilin Province of China (No. JJKH20210527KJ) and the Natural Science Foundation of the Jilin Province (No. 20210101407JC).

References

[1] S. J. Zhao, Z. Li, Z. Qu, N. Q. Yan, W. J. Huang, W. M. Chen, H. M. Xu, Co-benefit of Ag and Mo for the catalytic oxidation of elemental mercury, Fuel, 158 (**2015**), 891–897

[2] M. Özacar, A. S. Poyraz, H. C. Genuino, C. H. Kuo, Y. T. Meng, S. L. Suib, Influence of silver on the catalytic properties of the cryptomelane and Ag-hollandite types manganese oxides OMS-2 in the low-temperature CO oxidation, Appl. Catal. A, 462–463 (**2013**), 64–74

[3] H. Mao, C. G. Ji, M. H. Liu, Z. Q. Cao, D. Y. Sun, Z. Q. Xing, X. Chen, Y. Zhang, X. M. Song, Enhanced catalytic activity of Ag nanoparticles supported on polyacrylamide/polypyrrole/graphene oxide nanosheets for the reduction of 4-nitrophenol, Appl. Surf. Sci., 434 (**2018**), 522–533

[4] A. Ahmad, F. Ali, Z. A. Alothman, R. Luque, UV assisted synthesis of folic acid functionalized ZnO–Ag hexagonal nanoprisms for efficient catalytic reduction of Cr^{+6} and 4-nitrophenol, Chemosphere, 319 (**2023**), 137951

[5] K. Sawabe, T. Hiro, K. Shimizu, A. Satsuma, Density functional theory calculation on the promotion effect of H_2 in the selective catalytic reduction of NO_x over Ag–MFI zeolite, Catal. Today, 153 (**2010**) 3–4, 90–94

[6] S. Kundu, W. Dai, Y. Y. Chen, L. Ma, Y. Yuan, M. Sinyukov Alexander, L. Hong, Shape-selective catalysis and surface enhanced Raman scattering studies using Ag nanocubes, nanospheres and aggregated anisotropic nanostructures, J. Colloid Interface Sci., 498 (**2017**), 248–262

[7] T. Gan, Z. K. Wang, Z. X. Shi, D. Y. Zheng, J. Y. Sun, Y. M. Liu, Graphene oxide reinforced core–shell structured Ag@Cu_2O with tunable hierarchical morphologies and their morphology–dependent electrocatalytic properties for bio-sensing applications, Biosens. Bioelectron., 112 (**2018**), 23–30

[8] Y. G. Wang, X. Y. Wang, B. Sun, S. C. Tang, X. K. Meng, Concentration-Dependent Morphology Control of Pt-coated-Ag Nanowires and Effects of Bimetallic Interfaces on Catalytic Activity, J. Mater. Sci. Technol., 32 (**2016**) 1, 41–47

[9] C. R. Zhang, L. F. Wang, C. U. Dong, W. J. Zhu, W. H. Ge, Preparation of hollow Ag/Pt heterostructures on TiO_2 nanowires and their catalytic properties, Appl. Catal. B, 180 (**2016**), 344–350

[10] D. Biswas, S. Mondal, A. Rakshit, A. Bose, S. Bhattacharyya, S. Chakraborty, Size and density controlled Ag nanocluster embedded MOS structure for memory applications, Mater. Sci. Semicond. Process., 63 (**2017**), 1–5

[11] E. Ramírez-Meneses, V. Montiel-Palma, M. A. Domínguez-Crespo, M. G. Izaguirre-Lope, E. Palacios-Gonzalez, H. Dorantes-Rosales, Shape- and size-controlled Ag nanoparticles stabilized by in situ generated secondary amines, J. Alloys Compd., 643 (**2015**), s51–s61

[12] H. Tigger-Zaborov, G. Maayan, Nanoparticles assemblies on demand: Controlled aggregation of Ag(0) mediated by modified peptoid sequences, J. Colloid Interface Sci., 508 (**2017**), 56–64

[13] Z. Chen, D. S. Jia, Y. Zhou, J. Hao, Y. Liang, Z. M. Cui, W. G. Song, In situ generation of highly dispersed metal nanoparticles on two-dimensional layered SiO_2 by topotactic structure conversion and their superior catalytic activity, Appl. Surf. Sci., 434 (**2018**), 1137–1143

[14] Y. Chi, L. Zhao, Q. Yuan, X. Yan, Y. J. Li, N. Li, X. T. Li, In situ auto-reduction of silver nanoparticles in mesoporous carbon with multifunctionalized surfaces, J. Mater. Chem., 22 (**2012**), 13571–13577

[15] H. Mao, C. G. Ji, M. H. Liu, Z. Q. Cao, D. Y. Sun, Z. Q, Xing, X. Chen, Y. Zhang, X. M. Song, Enhanced catalytic activity of Ag nanoparticles supported on polyacrylamide/polypyrrole/graphene oxide nanosheets for the reduction of 4-nitrophenol, Appl. Surf. Sci., 434 (**2018**), 522–533

[16] X. G. Liao, L. Zheng, Q. He, G. Li, L. Zheng, H. M. Li, T. Tian, Fabrication of Ag/TiO_2 membrane on Ti substrate with integral structure for catalytic reduction of 4-nitrophenol, Process Saf. Environ. Prot., 168 (**2022**), 792–799

[17] S. Mohammadzadeh, M. E. Olya, A. M. Arabi, A. Shariati, M. R. Khosravi Nikou, Synthesis, characterization and application of ZnO-Ag as a nanophotocatalyst for organic compounds degradation, mechanism and economic study, J. Environ. Sci., 35 (**2015**), 194–207

[18] M. K. Kim, P. S. Kim, J. H. Baik, I. S. Nam, B. K. Cho, S. H. Oh, DeNO_x performance of Ag/Al_2O_3 catalyst using simulated diesel fuel–ethanol mixture as reductant, Appl. Catal. B, 105 (**2011**) 1–2, 1–14

[19] S. Liu, X. D. Wu, D. Weng, R. Ran, Ceria-based catalysts for soot oxidation: a review, J. Rare Earths, 33 (**2015**) 6, 567–590

[20] Y. Shi, X. L. Zhang, Y. M. Zhu, H. L. Tan, X. S. Chen, Z. H. Lu, Core–shell structured nanocomposites Ag@CeO_2 as catalysts for hydrogenation of 4-nitrophenol and 2-nitroaniline, RSC Adv., 6 (**2016**), 47966–47973

[21] Y. Y. Wang, Y. Shu, J. Xu, H. Pang, Facile one-step synthesis of Ag@CeO_2 core–shell nanospheres with efficient catalytic activity for the reduction of 4-nitrophenol, CrystEngComm, 19 (**2017**), 684–689

[22] B. Y. Guan, L. Yu, J. Li, X. W. Lou, A universal cooperative assembly-directed method for coating of mesoporous TiO_2 nanoshells with enhanced lithium storage properties, Sci. Adv. Mater., 2 (**2016**), 1501554

[23] Z. H. Wang, H. F. Fu, Z. W. Tian, D. M. Han, F. B. Gu, Strong metal–support interaction in novel core–shell Au–CeO_2 nanostructures induced by different pretreatment atmospheres and its influence on CO oxidation, Nanoscale, 8 (**2016**), 5865–5872

[24] Y. Chi, Q. Yuan, Y. J. Li, J. C. Tu, L. Zhao, N. Li, X. T. Li, Synthesis of Fe_3O_4@SiO_2-Ag magnetic nanocomposite based on small-sized and highly dispersed silver nanoparticles for catalytic reduction of 4-nitrophenol, J. Colloid Interface Sci., 383 (**2012**), 96–102

[25] J. S. Fang, Y. W. Zhang, Y. M. Zhou, S. Zhao, C. Zhang, H. X. Zhang, X. L. Sheng, In-situ formation of supported Au nanoparticles in hierarchical yolkshell CeO_2/mSiO_2 structures as highly reactive and sinter-resistant catalysts, J. Colloid Interface Sci., 488 (**2017**), 196–206

[26] C. Lee, J. Park, Y. G. Shul, H, Einaga, Y. Teraoka, Ag supported on electrospun macro-structure CeO_2 fibrous mats for diesel soot oxidation, Appl. Catal. B, 174–175 (**2015**), 185–192

[27] J. H. Yang, J. Wang, X. Y. Li, D. D. Wang, H. Song, Synthesis of urchin-like Fe_3O_4@SiO_2@ZnO/CdS core–shell microspheres for the repeated photocatalytic degradation of rhodamine B under visible light, Catal. Sci. & Technol., 6 (**2016**), 4525–4534

[28] L. Yu, R. S. Peng, L. M. Chen, M. L. Fu, J. L. Wu, D. Q. Ye, Ag supported on CeO_2 with different morphologies for the catalytic oxidation of HCHO, Chem. Eng. J., 334 (**2018**), 2480–2487

[29] L. Ma, D. S. Wang, J. H. Li, Ag/CeO_2 nanospheres: efficient catalysts for formaldehyde oxidation, Appl. Catal. B, 148–149 (**2014**), 36–43

[30] W. J. Deng, D. H. Chen, L. Chen, Synthesis of monodisperse CeO_2 hollow spheres with enhanced photocatalytic activity, Ceram. Int., 41 (**2015**), 11570–11575

[31] W. W. Zhang, D. H. Chen, Preparation and performance of CeO_2 hollow spheres and nanoparticles, J. Rare Earths, 34 (**2016**) 3, 295–299

[32] J. Zhang, M. Gong, C. Tian, C. A. Wang, Facile synthesis of well-defined CeO_2 hollow spheres with a tunable pore structure, Ceram. Int., 42 (**2016**), 6088–6093

[33] Y. Y. Wang, Y. Shu, J. Xu, H. Pang, Facile one-step synthesis of Ag@CeO_2 core–shell nanospheres with efficient catalytic activity for the reduction of 4-nitrophenol, CrystEngComm, 19 (**2017**), 684–689

[34] K. Vasanth Kumar, K. Porkodi, F. Rocha, Langmuir–Hinshelwood kinetics – A theoretical study, Catalysis Communications, 9 (**2008**) 1, 82–84

[35] L. E. Wu, S. M. Fang, L. Ge, C. C. Han, P. Qiu, Y. J. Xin, Facile synthesis of Ag@CeO_2 core–shell plasmonic photocatalysts with enhanced visible-light photocatalytic performance, J. Hazard. Mater., 300 (**2015**), 93–103